MCB
Journals.ASM.org

Analysis of Chromatin Dynamics during Glucocorticoid Receptor Activation

Craig J. Burd,[a] James M. Ward,[b] Valerie J. Crusselle-Davis,[a] Grace E. Kissling,[c] Dhiral Phadke,[d] Ruchir R. Shah,[d] and Trevor K. Archer[a]

Chromatin and Gene Expression Group, Laboratory of Molecular Carcinogenesis, National Institute of Environmental Health Sciences, National Institutes of Health, Department of Health and Human Services, Research Triangle Park, North Carolina, USA[a]; Integrative Bioinformatics Resource, National Institute of Environmental Health Sciences, Research Triangle Park, North Carolina, USA[b]; Biostatistics Branch, National Institute of Environmental Health Sciences, Research Triangle Park, North Carolina, USA[c]; and SRA International, Durham, North Carolina, USA[d]

Steroid hormone receptors initiate a genetic program tightly regulated by the chromatin environment of the responsive regions. Using the glucocorticoid receptor (GR) as a model factor for transcriptional initiation, we classified chromatin structure through formaldehyde-assisted isolation of regulatory elements (FAIRE). We looked at dynamic changes in FAIRE signals during GR activation specifically at regions of receptor interaction. We found a distribution of GR-responsive regions with diverse responses to activation and chromatin modulation. The majority of GR binding regions demonstrate increases in FAIRE signal in response to ligand. However, the majority GR-responsive regions shared a similar FAIRE signal in the basal chromatin state, suggesting a common chromatin structure for GR recruitment. Supporting this notion, global FAIRE sequencing (seq) data indicated an enrichment of signal surrounding the GR binding site prior to activation. Brg-1 knockdown showed response element-specific effects of ATPase-dependent chromatin remodeling. FAIRE induction was universally decreased by Brg-1 depletion, but to varying degrees in a target specific manner. Taken together, these data suggest classes of nuclear receptor response regions that react to activation through different chromatin regulatory events and identify a chromatin structure that classifies the majority of response elements tested.

Nuclear receptors are a superfamily of transcription factors that initiate specific genetic programs important in virtually all physiological processes, including development, metabolism, differentiation, and growth (12). Activity of the receptors is induced by ligands specific for each family member. After ligand activation, receptors translocate to the nucleus and dimerize on specific response elements within the genome (22). Upon target binding, nuclear receptors are then able modulate gene output by the recruitment of cofactors and transcriptional machinery (1, 42). This stepwise model of transcriptional regulation by nuclear receptors is regulated at various stages throughout the activation process.

The organization of chromatin structure provides an impediment to DNA-protein interactions that has been demonstrated to be a critical regulator of nuclear receptor recruitment to its target response element as well as transcriptional activation of target genes. Model transcriptional systems, such as the mouse mammary tumor virus (MMTV) promoter, have been invaluable in gaining an understanding of the critical role chromatin plays in nuclear receptor mediated gene transcription (45). Upon DNA binding by the receptor, cofactors are recruited to the promoter to alter chromatin structure and loosen DNA-histone interactions. The first class of cofactors possess enzyme activity that alters posttranslational modifications on the histone proteins (40). The best-characterized cofactors within this group are the histone acetyltransferases (HATs) and methyltransferases (KMTs), which acetylate or methylate histone tails within the core nucleosome particle critical for transcriptional initiation (26, 46). The second class of cofactors utilize the hydrolysis of ATP to actively remodel chromatin structure (29, 30). The SWI/SNF complex of chromatin remodelers has been very well characterized for its importance in nuclear-receptor-mediated transcriptional initiation (28, 36, 44). In fact, absence of the core ATPase subunit of the SWI/SNF complex results in decreased DNA accessibility, as measured by nuclease sensitivity assays, of the MMTV promoter upon glucocorticoid receptor (GR) activation (37). Furthermore, the importance of chromatin as a regulatory mechanism of the transcriptional process is validated by the fact that transiently transfected reporter constructs that fail to incorporate into a normal chromatin structure no longer need chromatin-remodeling factors such as SWI/SNF for activation (13, 25). Together these cofactors are believed to manipulate the chromatin structure, providing open and accessible DNA for the transcriptional machinery. Thus, a model of inaccessible DNA being modified by receptor binding and cofactor recruitment to generate an "open" or accessible locus has been hypothesized for transcriptional activation (17).

Recent characterizations of chromatin structure at nuclear receptor interacting regions using whole-genome approaches has indicated that the underlying basal structure at response elements plays an important role in determining cell specificity of receptor action (43). Whole-genome DNase sensitivity assays indicate that the majority of GR binding locations are constitutively nuclease accessible (21). Furthermore, comparison of lung to pituitary rat cell lines demonstrated that this accessibility was not only cell type specific but also correlated to the specific GR binding profiles. Examination of chromatin structure in human breast cancer cells

Received 30 August 2011 **Returned for modification** 3 November 2011
Accepted 6 March 2012
Published ahead of print 26 March 2012
Address correspondence to Trevor K. Archer, archer1@niehs.nih.gov.
Supplemental material for this article may be found at http://mcb.asm.org/.

doi:10.1128/MCB.06206-11

using formaldehyde-assisted isolation of regulatory elements (FAIRE) revealed a similar phenomenon. FAIRE utilizes DNA-protein cross-linking followed by phenol-chloroform extraction to differentially segregate regions of the genome, theoretically determined by the amount of histone-DNA contacts able to be cross-linked (15, 16). In the case of the estrogen receptor (ER), the ER pioneering factor, FOXA1, is associated in a cell-type-specific manner with open regions of the chromatin linked to nuclear receptor recruitment (11). Pioneering factors like FOXA1 and NF1 have been linked to the activity of numerous transcription factors, including the GR (4, 18, 35). These studies indicate that nuclear receptor specificity may be determined by underlying mechanisms such as pioneering factors that open chromatin at potential response elements in a cell-type-specific manner (8).

In this study, we aimed to utilize the FAIRE technique to assess chromatin during the dynamic process of GR activation. We analyzed FAIRE-enriched DNA prior to and following treatment with the GR ligand dexamethasone at specific receptor response elements. We further analyzed the chromatin structure using assays to determine nucleosome occupancy and DNase accessibility. Finally, we investigated the importance of ATPase-dependent remodeling for the chromatin dynamics of GR activation. This represents the first use of FAIRE to study a dynamic chromatin-remodeling process, and the data suggest a predominantly basal chromatin state for responsive genomic regions.

MATERIALS AND METHODS

Cell culture. A1-2 cells were described previously and were cultured in Dulbecco's modified Eagle medium (DMEM) containing 10% fetal bovine serum (FBS) containing 250 μg/ml G418 (3). A1-A3 cells were generated by transducing A1-2 cells with lentivirus containing a doxycycline (DOX)-inducible short-hairpin RNA (shRNA) construct targeting hBrg-1 (clone ID V2THS_153152; Open Biosystems). Cells were selected using 1 μg/ml puromycin, and the A1-A3 cell line represents the colony demonstrating the strongest knockdown of Brg-1 expression.

Immunoblotting. Cells were harvested and subjected to sodium dodecyl sulfate-polyacrylamide gel electrophoresis (SDS-PAGE) followed by immunoblotting using Brg-1 (SC-10768; Santa Cruz), β-actin (AB20272; Abcam), and GR (SC-1004; Santa Cruz) antibodies as previously described (6).

Transcriptional profiling. A1-2 cells were cultured in MEM containing 5% charcoal dextran-treated (CDT) serum for 48 h. Cells were then treated with either 100 nM dexamethasone or ethanol vehicle for 8 h. Total RNA was then harvested using a TRIzol Plus kit (Invitrogen) as described in the manufacturer's protocol. Gene expression analysis was conducted at the NIEHS microarray core using whole-human-genome 4-by-44 multiplex-format oligonucleotide arrays (014850; Agilent Technologies) following the Agilent one-color microarray-based gene expression analysis protocol. Agilent Feature Extraction software performed error modeling, adjusting for additive and multiplicative noise. The resulting data were processed using the Rosetta Resolver system (version 7.2) (Rosetta Biosoftware, Kirkland, WA).

Chromatin immunoprecipitation (ChIP). A1-2 and A1-A3 cells were cultured in MEM containing 5% CDT serum (MEM-CDT) for 48 h. A1-A3 cells were cultured in DMEM for 24 h with or without DOX prior to culture in MEM-CDT. Cells were then treated with 100 nM dexamethasone or ethanol vehicle for 1 h followed by ChIP analysis as previously described (38). For histone occupancy ChIP experiments, DNA was cleaved by addition of micrococcal nuclease as previously described (7). Cross-linked complexes were immunoprecipitated with antibodies directed against IgG control (SC-8998; Santa Cruz), GR (SC-1004; Santa Cruz), histone H3 (05-928; Millipore), or histone H2A (AB15653; Abcam). For receptor binding, purified DNA was quantified using a Qubit system (Invitrogen) per the manufacturer's instructions, and equal amounts of DNA were analyzed by real-time PCR with the indicated primer sets. For histone occupancy, equal volumes of purified DNA were analyzed as a percentage of input using real-time PCR with the indicated primer sets. Statistical significance was determined using a two-tailed paired *t* test.

FAIRE. Cells were cultured and treated with hormone as described above. Following hormone treatment, cells were cross-linked by the addition of formaldehyde to 1% for 5 min and then quenched with the addition of glycine to 125 mM. Following repeated phosphate-buffered saline (PBS) washing, cell pellets were lysed in FAIRE lysis buffer (2% Triton X-100, 1% SDS,100 mM NaCl, 10 mM Tris-Cl [pH 8.0], 1 mM EDTA buffer, 1× Sigma protease inhibitor cocktail) and sonicated with a Bioruptor (Diagenode) for 15 min at medium intensity. Lysates were then spun at 20,000 × *g* for 10 min at 4°C to remove cellular debris. Supernatant lysate (10%) was then collected as the input and treated with 10 μg proteinase K overnight at 40°C. The remaining lysate was then extracted with phenol chloroform and centrifuged to separate the aqueous phase, which was collected and saved. An additional 500 μl of Tris-EDTA buffer (TE) was then added to the phenol layer, mixed thoroughly, and centrifuged. The aqueous layer was collected, and the two samples were combined, followed by addition of 500 μl phenol-chloroform. The sample was centrifuged and the aqueous layer collected. DNA was precipitated by the addition of 1/10 volume sodium acetate (pH 5.3) and 2 volumes ethanol. DNA pellets were dissolved in TE, and inputs were then incubated overnight at 65°C to reverse the cross-links. DNA was then purified using a Qiagen PCR purification kit. Purified DNA was quantified, analyzed by real-time PCR using the appropriate primer sets (see Table S1 in the supplemental material) as a percentage of inputs, and then corrected for loading by nonspecific control that was reproducibly demonstrated not to be modulated by hormone treatment (data not shown).

For whole-genome analysis, next-generation sequencing libraries of FAIRE-enriched DNA were generated and sequenced on an Illumina IIx genome analyzer platform as previously described (16). Sequencing was performed in two phases, which yielded a total of about 70.3 million reads (reads were 36 nucleotides and 40 nucleotides long in phase 1 and phase 2 of sequencing, respectively). We performed sequence alignment of the roughly 70.3 million reads with the human genome (hg18) using Bowties with standard parameters (23, 24) and utilized approximately 42.2 million reads that uniquely aligned for further analysis. To calculate average FAIRE signal across all GR binding sites, we first defined genomic intervals corresponding to a ±1-kb window centered at previously defined GR peaks (32). For each of these genomic intervals, we then computed the number of reads aligned at each of the 2,000 nucleotides covered within the interval and calculated an average signal for each nucleotide across all sites. The average signal was recorded in reads per million (RPM). Thirty GR binding regions out of the total 15,847 identified peaks were removed due to their proximity to regions of the genome that result in unusually high read numbers, as determined by sequencing of T47D input DNA (data not shown). To generate a heat map displaying the FAIRE signal at each of the GR binding sites, we first defined 200-bp bins centered at GR peak locations. For each GR binding site, we computed average FAIRE signal (average number of reads aligning within the 200-bp bin) for each bin and clustered via a centered weighted row sum using R (31). Data are archived at the NCBI Sequence Read Archive (SRA) under accession no. SRA044977.

DNase sensitivity assays. A1-2 cells were cultured as previously described and treated with dexamethasone for 1 h. Cells were then collected in cold PBS. Nucleus isolation and DNase digestion were performed as previously described, with modifications (5). Nuclei were isolated by incubation for 10 min on ice with 5 ml Dounce buffer (20 mm Tris-HCl [pH 7.4], 3 mm $CaCl_2$, 2 mm $MgCl_2$, 0.3% Nonidet P-40, 1× Sigma protease inhibitor cocktail, 0.15 mM spermine, 0.5 mM spermidine) followed by Dounce homogenization. Nuclei were pelleted by centrifugation at 200 × *g* for 7 min. Nuclei were washed twice in resuspension buffer (10 mM

Tris-HCl [pH 7.4], 10 mM NaCl, 3 mM $MgCl_2$, 0.15 mM spermine, 0.5 mM spermidine) and pelleted by centrifugation at 200 × *g* for 7 min. Nuclei were then resuspended in 1 ml resuspension buffer, and nuclei were counted. Additional resuspension buffer was used to generate equal concentrations of nuclei between samples. Nuclei were aliquoted into microcentrifuge tubes and incubated at 37°C for 5 min. One unit of DNase was added to each of the aliquoted samples with the exception of the uncut control, and the samples were incubated at 37°C. Digestion was stopped at the time points indicated in Fig. 3 by addition of an equal volume of termination buffer (20 mM Tris [pH 7.4], 200 mM NaCl, 2 mM EDTA, 1% SDS, 200 μg/ml proteinase K). Reaction mixtures were incubated overnight at 37°C, followed by two phenol-chloroform extractions and one chloroform extraction of the DNA. DNA was quantified on a Qubit analyzer (Invitrogen), and equal amounts of DNA were analyzed by real-time PCR using the appropriate primer sets.

Microarray data accession number. The raw microarray data can be accessed through the Gene Expression Omnibus via the accession number GSE30592.

RESULTS

FAIRE analysis of glucocorticoid receptor activation. It is well demonstrated that recruitment of nuclear receptors to their target hormone response elements initiates numerous chromatin-modifying events that are required for transcriptional initiation. Model gene promoters, such as MMTV, show that chromatin-remodeling events that open chromatin allow access to the transcriptional machinery (2, 39). We thus aimed to analyze the molecular dynamics of chromatin reorganization during the process of GR activation. We utilized the A1-2 cell line, which is derived from the breast cancer T-47D cell line and contains both an MMTV luciferase reporter and a rat GR expression cassette (3). We chose 54 GR-interacting regions identified in A1-2 cells through ChIP sequencing (seq) experiments following 18 h of hormone treatment (unpublished data). As our interest was in the immediate chromatin-remodeling events that occur prior to and upon initiation of hormone signaling, we validated by chromatin immunoprecipitation GR binding at all 54 sites following 1 h of treatment with 100 nM DEX or ethanol vehicle (Fig. 1A). As can be seen, the increase in recruitment of DEX-activated GR over that of ethanol vehicle varied across all 54 sites, with some showing little to no response at 1 h (Fig. 1A). We set a minimum requirement of 30% enhanced GR signal upon DEX treatment as a categorical requirement of GR recruitment (Fig. 1A). Within the 54 tested sites, we verified GR recruitment at 40 sites at the 1-h time point. Interestingly, the vast majority of nonresponsive GR regions (11/14) were sites that did not contain a full glucocorticoid response element (GRE). In contrast, a large contingent of responsive regions contained full GREs (33/40). As all sites were identified by ChIP-seq following 18 h of ligand exposure, this suggests that many of the nonclassical responsive regions may act under different temporal dynamics.

We then utilized FAIRE to analyze the chromatin state at all 54 regions and an additional 4 transcriptional start sites (TSS) of hormone-responsive genes. A1-2 cells were treated for 1 h with DEX or ethanol vehicle, and FAIRE-enriched DNA was analyzed by quantitative real-time PCR. The change in activation of GR-responsive regions varied between none and ~6-fold induction of FAIRE signal following hormone treatment (Fig. 1B). Regions that were categorized as nonbinding for GR at the 1-h time point were utilized as a control and universally showed no change in FAIRE signal upon dexamethasone stimulation (Fig. 1B). Transcriptional start sites of genes that are responsive to hormone signaling also showed no induction of FAIRE signal upon GR activation (data not shown). We thus wanted to investigate if the strength of GR recruitment seen in ChIP analysis correlated with the chromatin reorganization observed in the FAIRE assays (see Table S2 in the supplemental material). The scatterplot utilizing these two variables across all 54 sites illustrates two points. First, nonresponsive control regions identified by ChIP cluster as nonresponsive in FAIRE (Fig. 1C). Second, removal of an outlier (NFKBIa 700 [Fig. 1C]), defined through a Grubb test of GR ChIP binding, allows a significant correlation ($P = 0.0138$) to be made between GR binding and fold induction of FAIRE signal following DEX treatment. As the majority of GR-responsive regions demonstrated a FAIRE-inducible signal, we investigated the dynamics of these chromatin-remodeling events over an 18-h time course. The FAIRE induction seen at two responsive sites occurs rapidly within 15 min of hormone signaling and is maximized 45 to 60 min following GR activation (Fig. 1D).

FAIRE signal induction parallels nuclease accessibility at GR-responsive regions. In order to assess whether FAIRE increases seen at GR-responsive regions were attributed to nucleosome removal, we performed ChIP assays using antibodies specific for histones H2A and H3. Histone H2A and H3 occupancy was lowest at TSSs, in concordance with the principle of nucleosome depletion within these regions (Fig. 2A). Regions that demonstrated the strongest FAIRE induction showed modest changes in histone occupancy (Fig. 2B). We observed similar profiles for regions that demonstrated FAIRE induction but with a lower initial FAIRE signal (Fig. 2C) or a relatively high initial FAIRE signal (Fig. 2D). Finally, a GR-responsive region that did not show a significant change in FAIRE signal following GR activation showed no changes in histone occupancy following hormone treatment (Fig. 2E). Overall, these data were consistent over multiple GR binding sites (data not shown) and suggest that GR recruitment does not result in nucleosome depletion, as a statistically significant change was observed only for one histone at one site. The largest change was observed in the histone H2A residence. To assess if these decreases were transitions to hexomes or specific exchanges of H2A isoforms, we performed ChIP for histones H2B and H2A.Z. We saw no change in histone H2B at any tested site (Fig. 2F). The site (FKBP5 6000) of the greatest histone H2A change showed an increase in H2A.Z residence, although it did not reach statistical significance ($P = 0.09$). These data together show no consistent loss of histone occupancy at GR binding sites following DEX treatment and suggest constant nucleosome residency.

We next examined the DNase sensitivity at GR-responsive sites to elucidate changes in chromatin architecture that allow the more open structure defined by our FAIRE signal. A1-2 cells were treated with DEX or ethanol vehicle for 1 h followed by nucleus isolation and DNase digestion. After isolation of digested DNA, cleavage surrounding GR-responsive sites was monitored by real-time PCR, and relative cleavage was measured by the ability of the polymerase to amplify regions around the response element. The value for undigested (0-min) DNA was set to 1 for each treatment, and the data represent the loss of amplification potential following DNase treatment for 2, 5, and 10 min. Regions that did not demonstrate GR binding or FAIRE changes showed identical DNase sensitivity between ethanol and DEX treatments (Fig. 3A). The CCNL1 region, which had a basal (ethanol) FAIRE signal of ~8, showed significantly more digestion than the LOC (LOC100131496) site, which had a relative FAIRE sig-

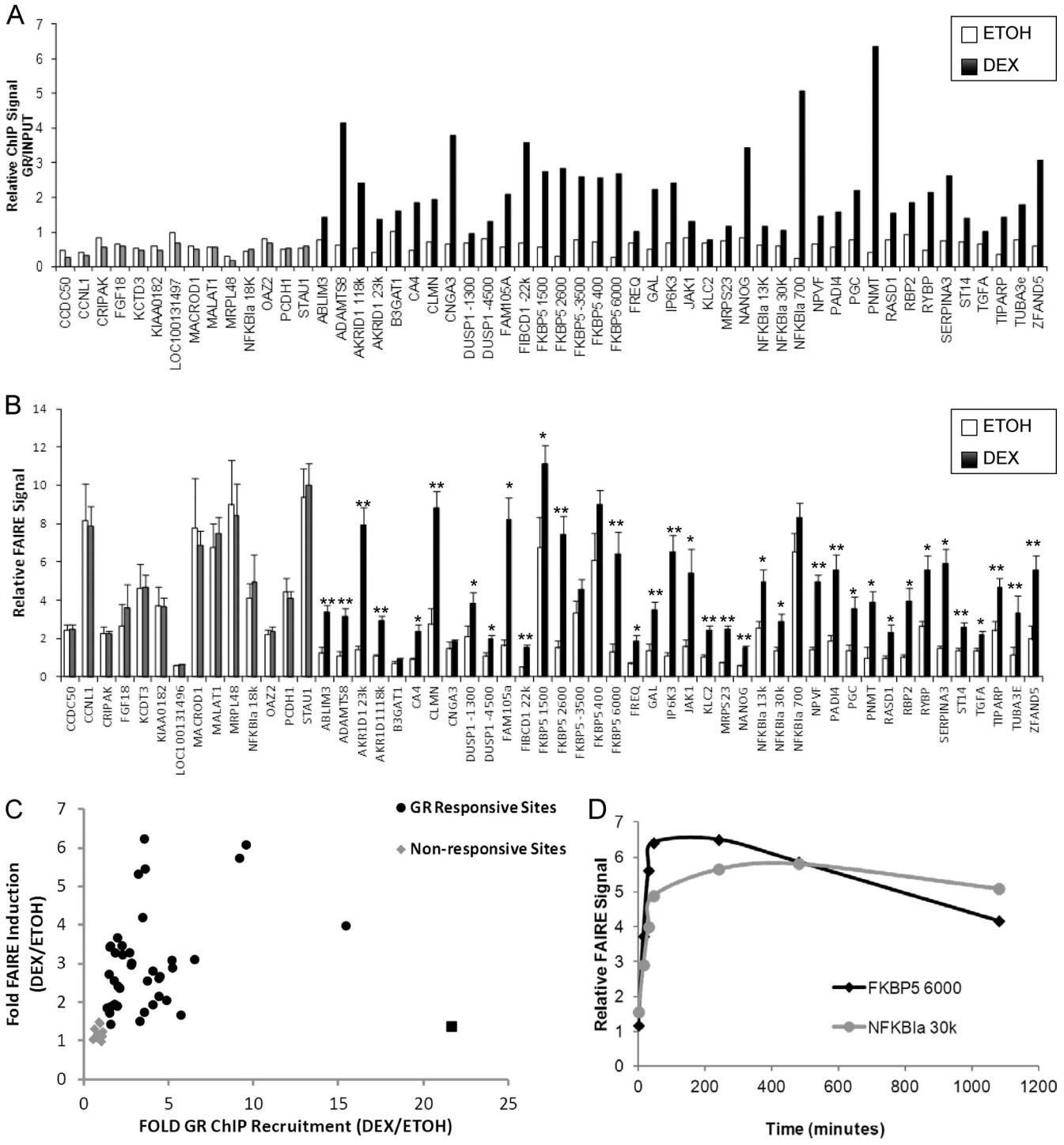

FIG 1 GR-responsive regions have varied chromatin-remodeling responses to receptor recruitment. (A) A total of 54 identified GR-responsive regions were tested for GR recruitment in A1-2 cells by ChIP analysis following 1 h of DEX treatment. Samples were analyzed by real-time PCR, and the graph shows the ChIP signal in ethanol vehicle- and DEX-treated samples after 1 h. Samples that did not demonstrate a minimum of 30% induction after GR activation were classified as not responsive (gray bars). The data are from one representative experiment of two replicates. (B) FAIRE analysis was performed on all 54 regions following 1 h of DEX treatment followed by real-time PCR analysis. The graph depicts the relative FAIRE signal at each locus in the presence of ethanol vehicle or DEX. Data are averages for a minimum of 4 biological replicates with standard errors; and regions determined for panel A not to have significant GR binding under these conditions are represented by gray bars. *, $P < 0.05$; **, $P < 0.01$. (C) Strength of GR binding, as determined for panel A, correlates with the induction of FAIRE signal, as determined for panel B. (D) Chromatin-remodeling events measured by FAIRE demonstrate rapid kinetics that are maintained for several hours after induction. A1-2 cells were treated with DEX, and samples were harvested at the indicated time points for FAIRE analysis. Samples were analyzed by real-time PCR using the indicated primer sets at genes that demonstrated significant increases in FAIRE signal at 1 h.

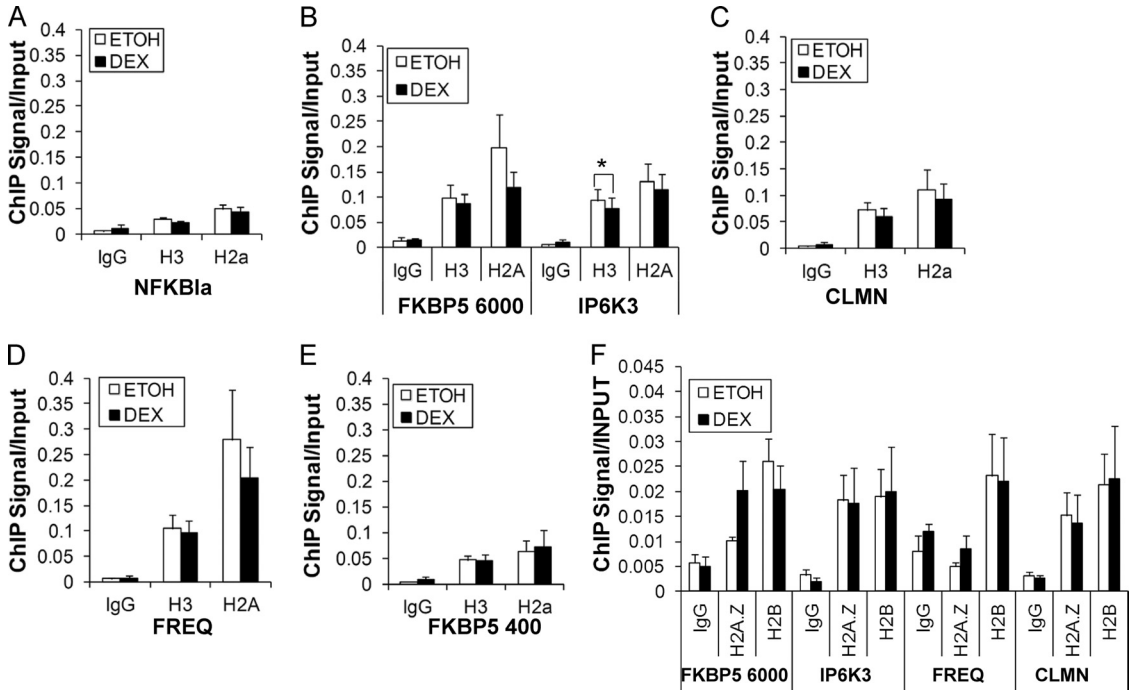

FIG 2 FAIRE induction does not indicate a loss of nucleosome occupancy at GR binding regions. A1-2 cells were treated with DEX or ethanol vehicle for 1 h, followed by ChIP analysis using antibodies specific for histone H3, histone H2A, and histone H3 lysine 4 trimethylation. Real-time PCR analysis was performed at a TSS of a GR-induced gene (A), regions that demonstrated a typical basal FAIRE signal that was significantly increase upon GR binding (B), a region that demonstrated no change in FAIRE upon GR binding (C), a region that showed high FAIRE signal that was also induced upon GR binding (D), and a region that showed very low FAIRE signal that was induced upon GR binding (E). Data are averages of 5 biological replicates with standard errors (*, $P < 0.05$). (F) ChIP assays were also performed with antibodies specific for histone H2B and H2A.Z at these regions.

nal of ~0.6. We then investigated the FKBP5 400 region, which did not demonstrate a significant FAIRE induction upon GR recruitment and likewise did not show any changes in DNase sensitivity (Fig. 3B). We then examined the two sites (FKBP5 6000, ~6.1; IP6K3, ~6.2) previously reported to have high FAIRE changes between DEX and ethanol treatments. These sites demonstrated an increased DNase sensitivity upon activation of GR (Fig. 3C). Both of these regions had relative FAIRE signals slightly higher than 1 under basal conditions. We then tested regions that demonstrated FAIRE induction but with high basal signals (CLMN, ~2.8) and low signals (FREQ, ~0.7). Both of these sites demonstrated increased DNase sensitivity that would be indicated by an increased FAIRE signal upon treatment with DEX (Fig. 3D and E). We also observe differences in overall DNase sensitivity indicative of the basal chromatin state. Sites that have relatively high FAIRE signals even in the absence of hormone, such as the CCNL1 and FKBP5 400 regions, demonstrated significantly more DNase sensitivity under all conditions than sites that have low FAIRE signals, such as the FREQ-responsive region. However, the sites that show large inductions of FAIRE signal (FKBP5 6000 and IP6K3, >6-fold) did not demonstrate greater changes in nuclease accessibility than sites that had smaller FAIRE inductions (CLMN, ~3.3-fold; FREQ, ~2.7-fold) when ethanol was compared to DEX treatments at any digestion time point (compare the 5-min digestion of IP6K3, FREQ, and CLMN). Thus, while FAIRE signal may generally correlate with changes in nuclease accessibility, alternate chromatin organization events may contribute to the FAIRE signal observed.

Chromatin reorganization events can be propagated to surrounding nucleosomes. As the majority of these sites demonstrated changes in chromatin architecture, we investigated if these remodeling events were specific for the immediate binding region or were more characteristic of multiple nucleosomal events. We thus investigated changes in FAIRE signal at regions downstream and upstream of the GR binding site. We utilized primers designed against regions roughly 500 bp upstream and 1,000 bp downstream of the FKBP5 6000 binding region as well as primers designed against regions 500 bp upstream, 300 downstream, and 800 downstream of the PNMT binding region (Fig. 4A). The FKBP5 6000 binding site typically shows ~6-fold FAIRE induction upon GR activation, and the regions flanking that site both upstream and downstream also demonstrated statistically significant FAIRE signal increases following hormone treatment even as far as 1,000 bp away from receptor recruitment (Fig. 4A). The PNMT region (~4-fold induction) also showed significant FAIRE induction 500 bp upstream of the GR binding location (Fig. 4A). The regions downstream of the PNMT binding site did not show a significant change but did demonstrate a higher FAIRE signal, indicative of those regions' proximity to the transcriptional start site. The FAIRE changes at these locations were all less than 2-fold, which is substantially lower than the changes at the nearby GR binding location. Nonetheless, significant FAIRE signal changes were consistent with an increased nuclease sensitivity following GR activation (Fig. 4B) at the regions 1,000 bp upstream and 500 bp downstream of FKBP5 binding location.

Chromatin reorganization as measured by FAIRE does not correlate with the strength of the transcriptional response. We next compared the strength of chromatin remodeling observed by FAIRE with the transcriptional response at target gene promoters. We utilized a microarray approach to characterize the transcrip-

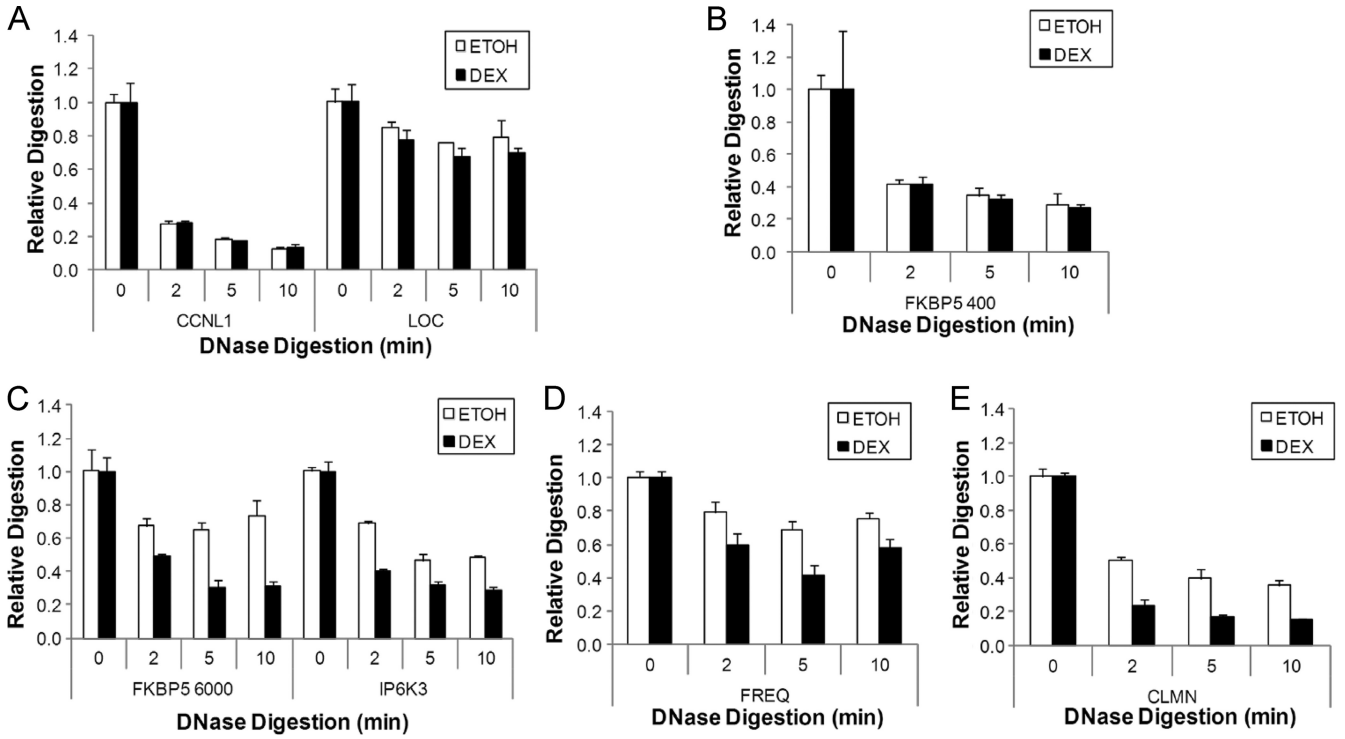

FIG 3 FAIRE signal and induction correlate with nuclease sensitivity. A1-2 cells were treated with DEX or ethanol vehicle for 1 h, followed by DNase treatment of isolated nuclei for the indicated time points. DNase sensitivity was measured by the ability to amplify regions surrounding GR binding locations described for Fig. 2 using real-time PCR. The data are from a representative experiment, and standard deviations of the technical replicates are shown.

tional response following 8 h of DEX treatment in A1-2 cells. This time frame allowed measurable transcriptional responses while minimizing secondary effects. Tested GR binding regions were then linked to the gene having the nearest transcriptional start site, and fold transcriptional change was calculated (see Table S2 in the supplemental material). We then aimed to compare the changes in FAIRE signal upon GR activation to the transcriptional response observed upon DEX treatment. There was no significant correlation between fold FAIRE induction and fold transcription change at the associated target gene. However, many genes contain multiple responsive elements, making the linkage between chromatin-remodeling events at any one locus and the transcriptional response for that gene difficult. However, within our 40 studied regions, 17 genes were identified that had only one mapped GR binding site. Examination of the transcriptional response and FAIRE induction using only these 17 binding sites still yielded no significant correlation and suggests that that the magnitude of chromatin-remodeling events does not determine the amount of transcriptional activity initiated by the receptor. We also investigated the transcriptional response at these 17 binding regions at a shorter transcriptional time point of 2 h and still yielded no significant correlation (data not shown). We finally investigated if the amount of GR ChIP signal correlated to transcriptional response at these 17 genes. No correlation was seen between the intensity of GR binding as measured by ChIP and the transcriptional changes observed in the closest gene.

GR-responsive regions have a similar basal chromatin signature. Across the 40 GR recruitment regions, we observed a diversified distribution of FAIRE signals. In an effort to understand factors that may contribute to this diversified response, we grouped the responsive regions based upon their distance from the nearest transcriptional start site. GR binding sites were categorized as being greater than 10 kb upstream, between 1.5 and 10 kb upstream, within 1.5 kb, between 1.5 and 10 kb downstream, and greater than 10 kb downstream of the transcriptional start site. Changes in FAIRE signal within these groups demonstrate that a response element's proximity to a transcriptional start site has no correlation with chromatin-remodeling events at that response element following receptor activation (Fig. 5A). However, the basal FAIRE signal in the uninduced state within these groups suggests that the greatest variance occurs near transcriptional start sites (Fig. 5B). Binding locations surrounding transcriptional start sites have a tendency to have higher FAIRE signals prior to receptor activation. This finding is consistent with the observation that FAIRE peaks are known to be found at transcriptional start sites which are often depleted of nucleosomes (15). However, FAIRE signatures at other regions of the genome are remarkably similar and are suggestive of a preferred chromatin architecture underlying GR-responsive regions.

To examine the role of the underlying chromatin structure on the GR response, we compared the uninduced FAIRE signal across all 40 binding sites to the changes in FAIRE signal observed upon receptor activation. We see a statistically significant correlation ($P = 0.039$) between basal FAIRE signal and changes induced by GR activation (Fig. 5C). Those sites with constitutively high FAIRE signal (>4) are relatively unresponsive to GR activation and localize near TSSs. However, the vast majority of GR binding regions have a lower FAIRE signal and cluster together based upon their uninduced FAIRE signal, which again suggests a preferred chromatin state for GR recruitment. However, that clustering is

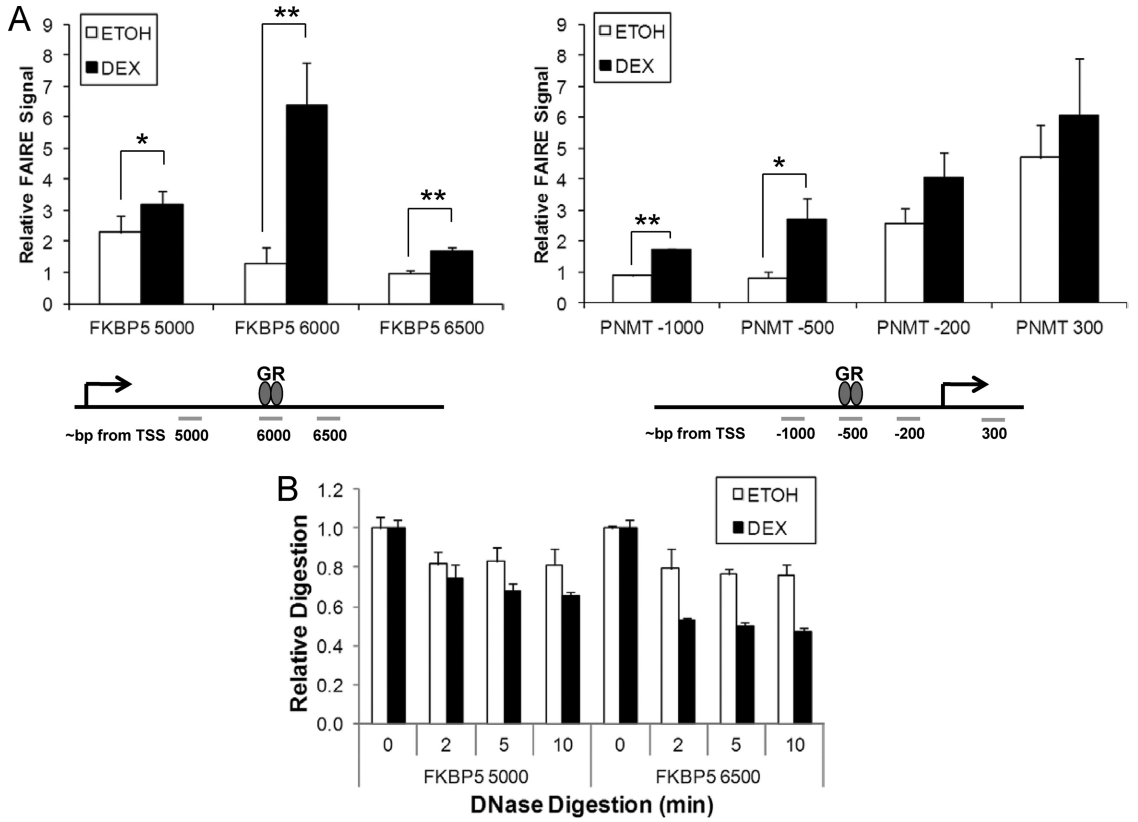

FIG 4 GR recruitment can initiate chromatin-remodeling events several nucleosomes from binding regions. (A) FAIRE experiments described for Fig. 1 were used to analyze regions adjacent to GR recruitment at the FKBP5 6000 (~6-fold FAIRE increase) and PNMT (~4-fold FAIRE increase) response elements. Data are averages for a minimum of 4 biological replicates with standard errors. *, $P < 0.05$; **, $P < 0.01$. (B) The regions surrounding the FKBP5 6000 response element were then tested for changes in DNase sensitivity as described for Fig. 3.

completely lost and the diversity of chromatin remodeling is observed when the induction is compared to the FAIRE signal after receptor activation (Fig. 5D). Taken together, responsive elements have a similar chromatin structure as measured by FAIRE prior to activation, but receptor recruitment results in a broad range of chromatin-remodeling events.

In order to better understand how a common basal underlying chromatin state may be seen at GR-responsive sites, we performed next-generation sequencing of FAIRE-enriched DNA from A1-2 cells under noninducing (ethanol vehicle) conditions using the Illumina GA IIx platform. Libraries from two biological replicates were created for sequencing, and the resulting sequence reads were combined for analysis following alignment to the University of California, Santa Cruz (UCSC), human reference genome (hg18). Roughly 42.2 million reads aligned uniquely out of the total 70.3 million sequences generated. We utilized previously published GR ChIP-seq data to analyze the FAIRE signal across the entire GR cistrome (32). Interestingly, there was an increase in FAIRE signal that corresponds to the roughly 15,000 GR peaks (Fig. 6A). This signal is specific for GR locations, as about an equal number (15,000) of randomly selected genomic loci demonstrated no FAIRE signal. We also scanned the genome for consensus glucocorticoid response elements by sequence and randomly selected 15,000 for analysis that were absent from the ChIP-seq binding set. These GREs lack the FAIRE signal seen at actual recruitment sites, suggesting that this FAIRE signature marks receptor binding potential. To ensure against genomic sequencing bias, we also utilized sequenced reads of input DNA from T47D cells across all GR binding locations. Regions of high sequencing in the T47D input DNA were mirrored in the T47D FAIRE sequencing data, and GR binding regions that were within 1,000 bp of high-read-number loci were removed from the analysis (30 binding regions). Furthermore, signal at the 40 GR peaks utilized in Fig. 1 to 5 display a signal profile very similar to that of all GR binding sites (Fig. 6B), suggesting that those sites are representative of the genomic set. The GR FAIRE peak observed in the FAIRE-seq data set is representative of most GR sites (67% greater than background), as can be seen on a heat map of all binding locations, and is not a result of a relatively small fraction of high-FAIRE-signal elements (Fig. 6C). These results clearly demonstrate that the increased signal is observed at most GR binding sites across the genome and that the increase in average signal adjacent to GR binding location is not dependent upon a select few highly enriched regions. As this signature is observed in the absence of glucocorticoids, it is completely independent of GR. PCR assessment of 40 sites depicted a generally closed state of chromatin prior to receptor activation and in comparison to TSSs. In contrast, analysis of the entire genome depicts FAIRE enrichment at the binding site prior to GR activation in comparison to random genomic loci. Thus, GR response elements have an intermediary FAIRE signal greater than that of the majority of the genome but significantly less than that of the activated site.

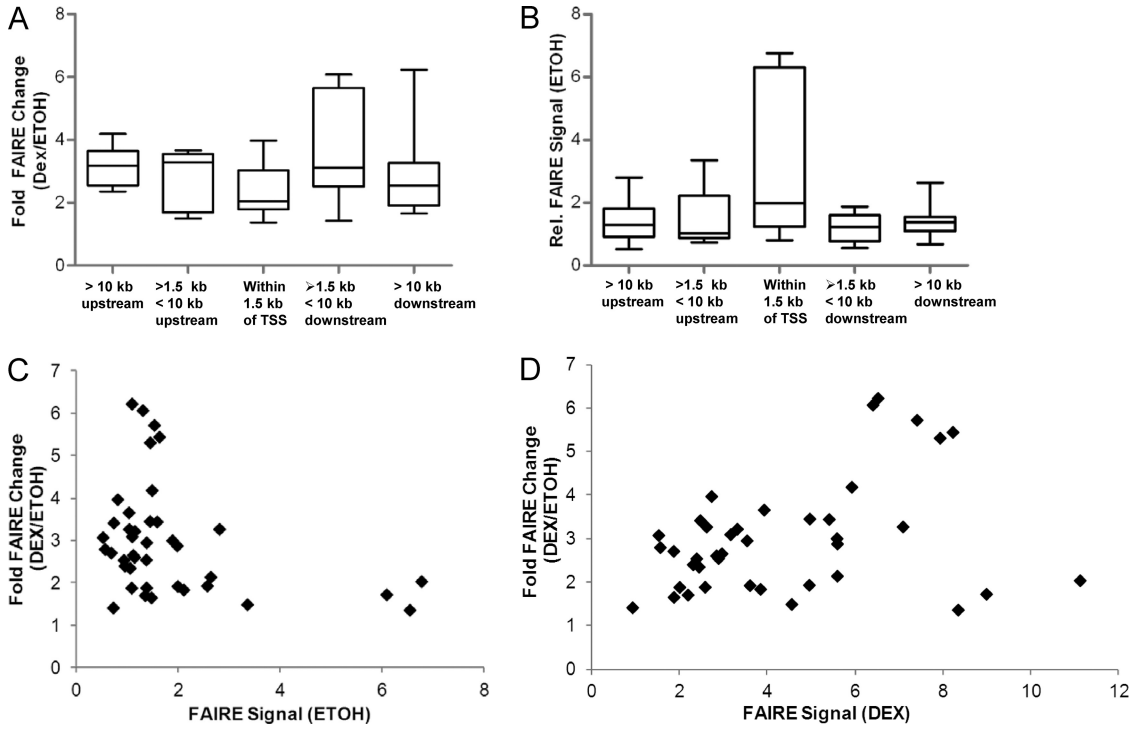

FIG 5 The majority of GR-responsive regions lie within a narrow window of chromatin openness, as measured by FAIRE. (A) The 40 GR-responsive regions were grouped based upon their distance from the nearest transcriptional start sites. Box-and-whisker plots of each group's fold FAIRE changes upon GR activation are shown. (B) Box-and-whisker plots of each group's basal FAIRE signal prior to GR activation. (C) Scatter plot of GR-responsive regions correlating ($P < 0.05$) the basal chromatin FAIRE signature to the ability of GR to induce changes in FAIRE signal. (D) Scatter plot of GR-responsive regions comparing the overall FAIRE signal after DEX induction to the amount of FAIRE signal induction.

In order to assess the basal FAIRE signal seen at GR binding regions in the absence of hormone, we performed bioinformatic analysis of the GR regions. We utilized the HMR Conserved Transcription Factor Binding Sites tool (http://genome.ucsc.edu/cgi-bin/hgTrackUi?hgsid=238139061&c=chr1&g=tfbsConsSites) from the UCSC Genome Browser to identify transcription factor binding sites within 900 bp of the GR recruitment location based upon the binned regions in Fig. 6C (see Table S3A in the supplemental material). We investigated enrichment of these transcription factors by normalizing against the total number of genomic binding events for each transcription factor (see Table S3B in the supplemental material). These analyses indicate that transcription factors have a high percentage of binding sites near GR binding regions. Reorganizing the sites based upon FAIRE signal within the GR binding bin, we investigated the potential role of transcription factor binding to basal chromatin structure at receptor recruitment sites. The sites were placed into quartiles, with quartile 1 having the lowest FAIRE signal in GR binding bin and quartile 4 having the highest FAIRE signal. Transcription factor binding for each bin was then normalized against the average number of sites found within the total GR set (see Table S4 in the supplemental material). The values represent the fold enrichment over the average binding events for all bins (1 = evenly dispersed). As expected, GR binding motifs are strongly enriched to the central bin across all quartiles. Interestingly, the central bin also showed the highest enrichment of other transcription factor binding sites, although no single transcription factor segregated to a specific quartile. We also utilized HOMER motif software discovery (http://biowhat.ucsd.edu/homer/index.html) to perform motif analysis on the GR binding regions by quartile (19). While a number of motifs, such as AP-1 and forkhead, were identified as being significantly enriched at GR binding sites, no single motif was unique for a specific quartile or FAIRE signature (see Table S5 in the supplemental material).

FAIRE-measured chromatin remodeling is dependent upon SWI/SNF. The SWI/SNF ATPase-dependent chromatin-remodeling complex has been shown to be critical for the activation of GR signaling at target promoters (13, 44). We thus wanted to determine if FAIRE changes observed at these target sites were dependent upon SWI/SNF function. We utilized an inducible shRNA system that targets the core ATPase subunit of the complex Brg-1. A1-2 cells were transduced with lentivirus containing the inducible system, and stable clones showing excellent knockdown of Brg-1 protein levels 72 h after shRNA induction with 10 μg/ml of DOX were selected (Fig. 7A). The transcriptional activity of GR following Brg-1 knockdown was determined by analyzing the integrated MMTV luciferase reporter system in these cells after 8 h of DEX treatment. The ability of GR to activate the MMTV reporter was greatly diminished under conditions of Brg-1 knockdown (Fig. 7B). Using the knockdown cells, we compared chromatin-remodeling events in the presence and absence of active SWI/SNF function using FAIRE. Cells were treated with DOX or vehicle for 72 h to achieve maximum knockdown of Brg-1 protein. Cells were then treated with 100 nM DEX or ethanol vehicle for 1 h followed by FAIRE analysis. Regions that did not demonstrate GR binding or FAIRE induction in A1-2 cells were unaffected by the depletion of Brg-1 (Fig. 7C). We then examined GR-respon-

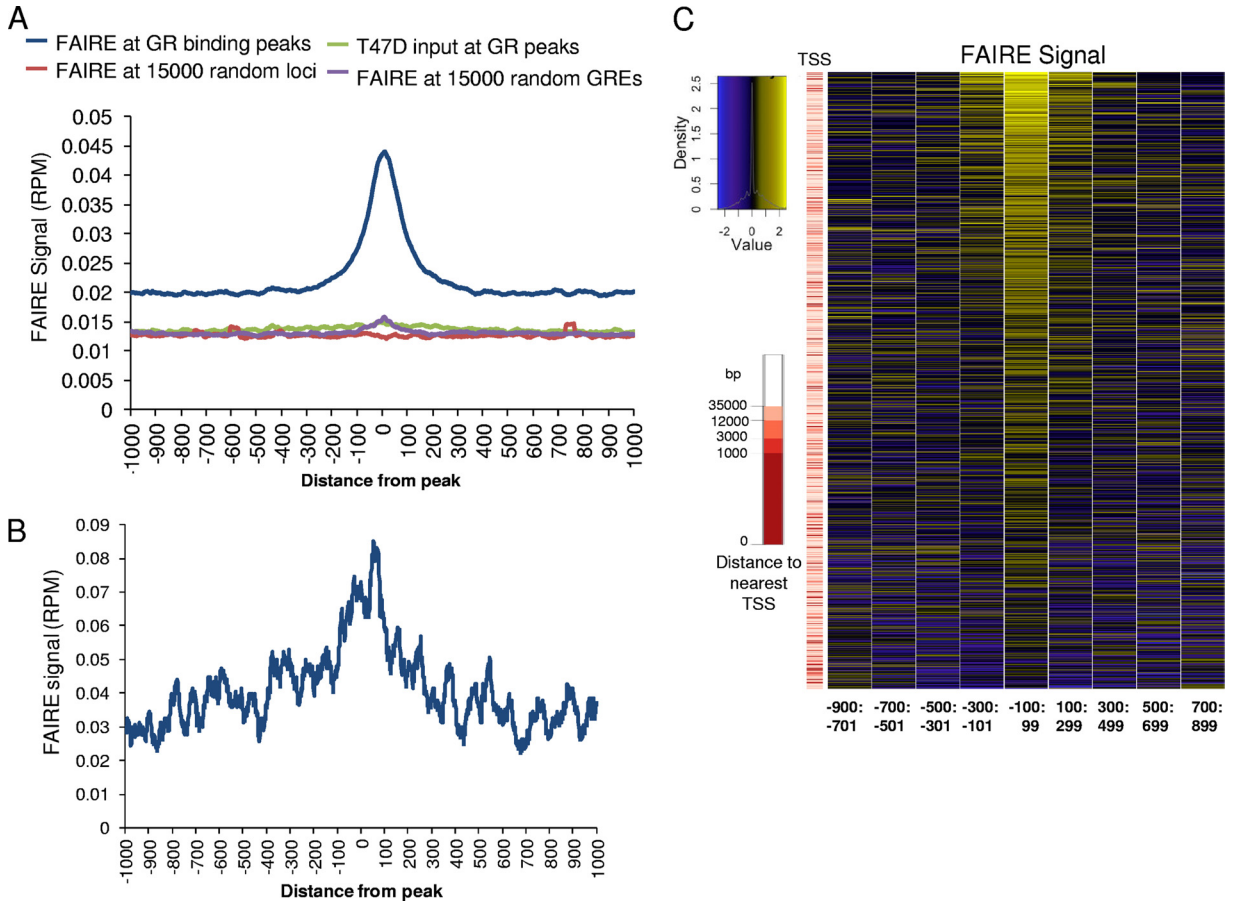

FIG 6 GR-responsive regions show an increased FAIRE signal across the whole genome. (A) Average FAIRE signals, determined from FAIRE-seq data, surrounding 15,816 GR binding regions and 15,000 random loci. A total of 15,000 random GREs absent from the ChIP-seq data show no FAIRE signal. Average input sequencing data from T47D cells are also included to ensure no sequencing bias. Average signal on the *y* axis is represented as RPM (reads per million sequences), where 0.1 RPM corresponds to 3 reads. (B) The average FAIRE-seq signal of the 40 GR-responsive sites from Fig. 1 shows a profile similar to that of the larger 15,000-data-point set. (C) FAIRE-seq data were placed in 200-bp bins surrounding 15,671 GR binding sites, and the heat map represents the FAIRE signal surrounding those GR binding peaks. Bins are marked by the distance (in bp) of the bin to the peak of the GR binding site. The additional strip (on left) represents the distance of the GR binding site to the closest TSS.

sive regions following depletion of Brg-1 protein and SWI/SNF activity. Induction of FAIRE by GR is abrogated by the loss of Brg-1 across all investigated inducible regions (Fig. 7D). Interestingly, despite the fact that these targets are analyzed from the same sample and thus have identical Brg-1 depletion, the response to Brg-1 knockdown is varied. While some GR-responsive sites have near complete ablation of FAIRE signal induction, others show only modest (roughly 35%) reduction. Brg-1 depletion had no effect on sites that were not induced upon GR recruitment. Interestingly sites adjacent to the GR regions that had demonstrated FAIRE induction (Fig. 4) demonstrated complete loss of that induction upon Brg-1 knockdown (Fig. 7E). Comparing 21 GR-responsive regions investigated upon Brg-1 knockdown, we found a statistically significant ($P < 0.0001$) decrease in FAIRE signal upon inactivation of the SWI/SNF complex (Fig. 7F). Taken together, these data demonstrate that SWI/SNF function contributes across virtually all chromatin-remodeling activities involved in GR activation.

DISCUSSION

The activation of transcription by nuclear receptors is a tightly controlled process regulated at the levels of ligand accessibility, cellular localization, cofactor availability, and finally chromatin architecture. It has been shown on several model promoters, such as MMTV, that both SWI/SNF activity and chromatin reorganization events are prerequisites for transcriptional initiation (13). Theoretically, chromatin remodeling is required to allow access of the transcriptional machinery. However, recent genomewide studies have indicated that specificity of nuclear receptor activity across various cell types is dictated by the presence of an open underlying chromatin structure surrounding the response element (11, 21). In the present study, we utilized FAIRE to assess chromatin dynamics prior to recruitment and following activation of GR. We were able to demonstrate that the majority of receptor-bound sites showed changes in FAIRE signal indicative of a more open chromatin structure and that this increase in signal correlates to GR binding. Nonetheless, FAIRE signal induction was dependent upon SWI/SNF activity at all responsive sites.

Chromatin remodeling following GR activation. Changes in chromatin structure following activation of nuclear receptors is a well-documented event believed to allow access of transcriptional machinery to the target promoter. Changes in histone modifications and nuclease sensitivity depict the opening of chromatin as

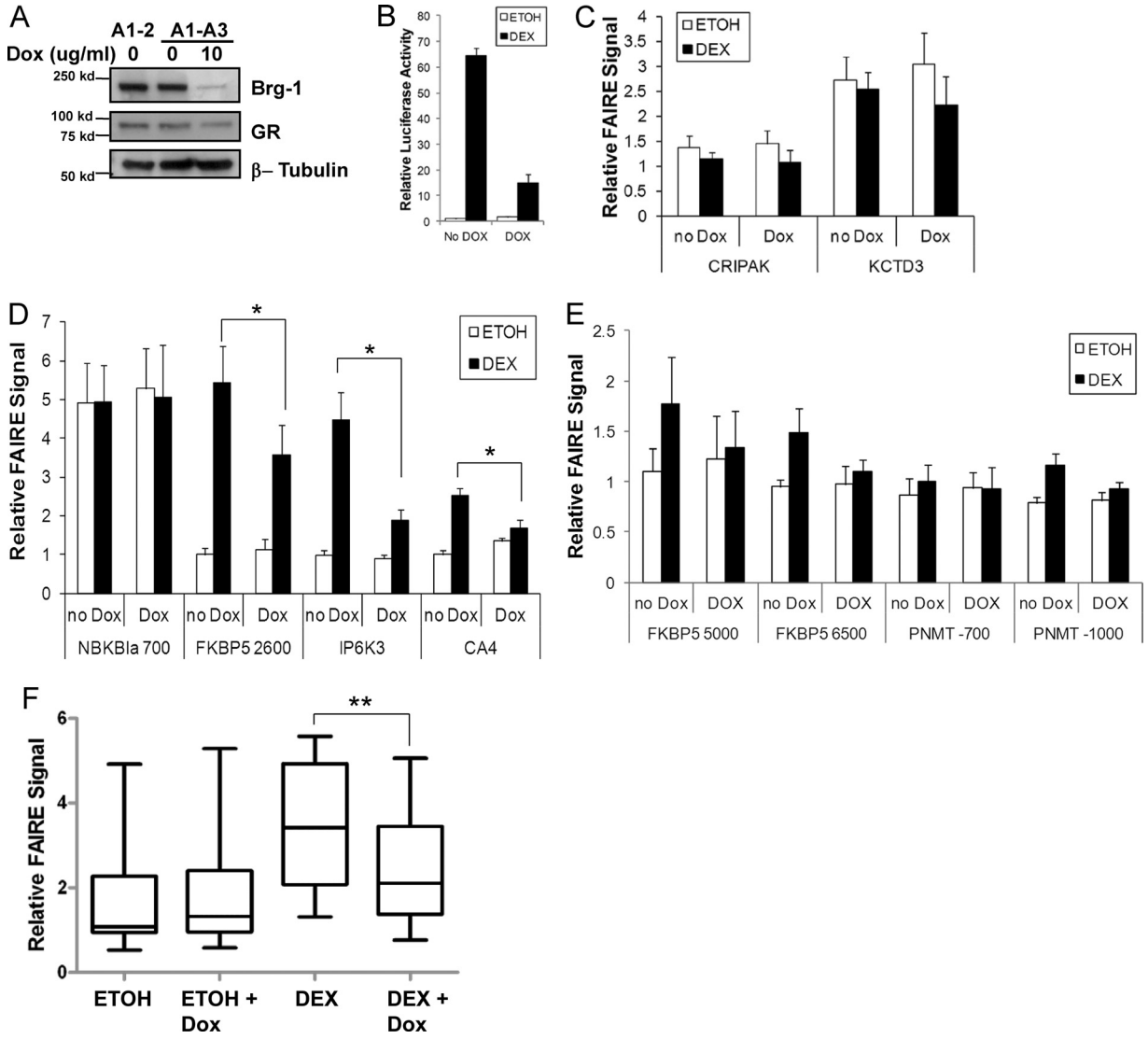

FIG 7 SWI/SNF function is critical for chromatin reorganization at most GR-responsive sites. (A) A1-2 cells were transduced with lentivirus containing an inducible shRNA targeting the ATPase subunit of the SWI/SNF complex, Brg-1. A stable clone, termed A1-A3, was generated and tested for Brg-1 knockdown following 72 h of shRNA induction by treatment with 10 μg/ml doxycycline. Knockdown was analyzed by immunoblotting cell lysates with antibodies specific for Brg-1. Expression of GR and β-actin was also analyzed. (B) A1-A3 cells were treated with 10 μg/ml DOX for 72 h followed by treatment with DEX or ethanol vehicle for 8 h. Cells were harvested, and lysates were analyzed for luciferase assay and total protein. Data are average relative luciferase activities (luciferase activity/total protein) for three biological replicates with standard deviations. (C to E) A1-A3 cells were treated for 72 h with 10 μg/ml doxycycline followed by treatment with DEX or ethanol vehicle for 1 h. Cells were then subjected to FAIRE analysis by real-time PCR using the indicated primer sets. Data are averages for four biological replicates with standard errors. *, $P < 0.05$. (F) Average FAIRE signals in A1-A3 cells of 21 GR-responsive regions in the presence and absence of DEX and Brg-1 (**, $P < 0.0001$).

an initiating occurrence following receptor recruitment. Open chromatin structure has further been demonstrated in real time using microscopy techniques to visualize the actual physical enlargement of promoters inherent to the decondensation of chromatin (34). Our data indicate that the vast majority of GR recruitment sites reorganize and open chromatin concurrently with receptor recruitment. Although SWI/SNF recruitment has been shown to cause nucleosome eviction, we did not see any measurable loss in histone H3 occupancy following GR activation (Fig. 2) (9). Analysis of nucleosome occupancy utilizing ChIP indicated very little change for the majority of histones (Fig. 2). In fact, only one site showed a statistically significant decrease in histone H3 occupancy (17%), and this site showed no changes in histone H2A or histone H2B. As no site showed a uniform decrease in histone ChIP signal, nucleosome presence is most likely constant. Most sites did show a small decrease in ChIP signal following DEX treatment that was not significant. These changes may be the result of decreased cross-linking efficiency of the histones to the DNA in the more open chromatin state. It also may indicate a decreased accessibility of the antibody to the target histone in the presence of GR and its coregulatory molecules. Interestingly, the largest change in histone occupancy following GR activation was seen at the FKBP5 6000 sites in which histone H2A decreased 40% following DEX treatment. It has been previously reported that nu-

clear receptor recruitment results in the exchange of isoforms, resulting in the incorporation of histone H2A.Z, which may not be recognized by the immunoprecipitating antibody (14, 20). The FKBP5 6000 region also demonstrated a twofold increase in histone H2A.Z occupancy. However, it did not appear that overall FAIRE signal or changes in signal were predictors of changes in histone H2A.Z exchange. Taken together, these data indicate that as GR binding regions maintained nucleosome occupancy at the site of FAIRE induction, changes in signal may reflect alterations in the ability of multiple compacted nucleosomal regions to cross-link and thus be an assessment of three-dimensional chromatin architecture.

Underlying chromatin structure and GR recruitment. Studies investigating nuclear receptor recruitment and activity have indicated that accessibility of the response element dictated by the chromatin structure is responsible for coordinating the specificity between different cell types (11, 21). These studies have indicated that pioneering factors which are believed to open chromatin prior to receptor recruitment are preferentially found at active sites between cell types. While we did find enrichment of alternate transcription factors and potential pioneering factors overlapping GR sites of recruitment, no motif correlated with higher FAIRE signal. This suggests that one single factor is not responsible for organizing the chromatin at potential binding regions. However, the prevalence of many transcription factor motifs in close proximity (100 bp) to the GR binding site compared to 100 to 900 bp from the binding site advocates very tight hotspots of transcription factor activity.

Pioneering factor recruitment is marked by open chromatin, as measured by FAIRE (11). In rat cell lines, specific GR recruitment is marked by constitutive DNase hypersensitivity, which is distinguished from the same site in an alternative cell line without GR recruitment (21). These studies have put forth a model in which the nuclear receptor specificity is defined by its access to the response element. However, this model is in contrast to many studies on model gene promoters where receptor recruitment is required prior to or concomitantly with chromatin reorganization and nuclease hypersensitivity (3, 10, 33). Using FAIRE to analyze the chromatin structure at GR binding sites, we found that the majority of receptor-responsive regions cluster together in the uninduced state. In contrast, the regions that did not bind GR had a much broader range, with the majority of signals being greater than the GR bound sites. We also observed FAIRE signals that were up to more than three times higher at transcriptional start sites, indicating the dynamic range of this assay. These data suggest that the majority of GR-responsive sites share similar chromatin characteristics and that this structure is relatively closed prior to receptor interaction compared to TSSs and following receptor recruitment. These data are in concert with the dogma that receptor-mediated chromatin-remodeling events are required to increase accessibility of transcriptional machinery. However, we did observe some DNase accessibility at sites characterized by this relatively low FAIRE signal (Fig. 3B and D). More importantly, there is an increase in FAIRE signal at GR binding regions across the entire genome, and that signal is significantly higher than that at randomly selected genomic loci (Fig. 6A) and unutilized response elements. This modest increase in signal is not dependent upon a small cohort of relatively high FAIRE signal sites but rather reflects a general trend of signal across all GR binding locations (Fig. 6B). Together, these data support the notion that responsive sites must have some degree of access for nuclear receptor recruitment and coincides with the notion that cell-type-specific regulation of the response elements is mediated through a more open chromatin structure. However, our analysis of specific promoters demonstrates a relatively low FAIRE signal compared to both transcriptional start sites and GR sites following recruitment. Furthermore, the FAIRE signal at the majority of these 40 sites indicated low DNase accessibility. As these specific promoters were representative of the genomic set (Fig. 6B), the term "constitutively open" response elements may be a misnomer. This phenomenon may require an alternate view of chromatin structure beyond the dichotomous open and closed dogma. In fact, our data suggest a transitional state between open and closed that allows receptor recognition. This state is more open than the majority of the genome but is still mostly inaccessible.

Chromatin-remodeling events following GR activation. The model of nuclear receptor activation involves the modification of chromatin by cofactors to allow transcriptional initiation. These cofactors act to either modify histone proteins or remodel chromatin structure through ATPase-dependent complexes. In fact, differential coregulator recruitment by selective estrogen receptor modifiers results in differential gene expression (27). This model of transcriptional regulation is not strictly nuclear receptor dependent but is rather a general phenomenon for inducible gene transcription. In line with this model, recent genomewide DNase mapping in rat cells following GR activation demonstrated that virtually all GR binding regions demonstrated increased accessibility following receptor recruitment (21). Our data obtained by using FAIRE to assess chromatin openness supports this model. Nearly, all of the tested regions demonstrated an increase in FAIRE signal following GR activation, although some did not meet statistical thresholds for significance. Interestingly, sites that demonstrated the highest basal FAIRE signal showed the least change in FAIRE signal. These sites, typically surrounding transcriptional start sites, are most likely constitutively open and thus do not require further remodeling. This phenomenon does not appear to be restricted to GR-responsive regions within 1.5 kb of transcriptional start sites, as other regions demonstrated significantly higher relative FAIRE signals as well.

The importance of ATPase-dependent chromatin remodeling in transcriptional initiation following receptor activation has been demonstrated for a number of model genes. SWI/SNF has also been implicated in maintaining the basal chromatin architecture required for GR binding and to allow loading of additional transcription factors and results in increased steady-state binding (20, 41). In our system, all sites that demonstrated FAIRE increases upon GR activation were suppressed upon Brg-1 knockdown. Interestingly, recent work has shown that in alternate systems, some GR-responsive sites may be SWI/SNF independent. This difference may be cell type specific or may be indicative of different experimental approaches. Specifically, the use of dominant negative Brg-1 to inhibit SWI/SNF activity may allow some scaffolding function that would be lost by knockdown. Loss of Brg-1 protein affected the FAIRE induction differently in a site-specific manner. While some targets showed nearly 100% loss of FAIRE induction, others demonstrated only a 35% loss (Fig. 7). These differences may be dependent upon alternate cofactors important in remodeling and modifying chromatin. Alternatively, some targets may be more proficient at recruiting residual active complexes following incomplete knockdown. Regardless, the role of the SWI/SNF

complex across targets is clearly variable. Interestingly, we also saw very little variation in the basal FAIRE signal upon loss of SWI/SNF. Only one site demonstrated a significant change in FAIRE signal upon Brg-1 depletion, which suggests that maintenance of a preferred GR chromatin architecture is thus not dependent upon SWI/SNF function.

The epigenetic mechanisms by which chromatin regulates transcriptional initiation are critical for determining the means by which biology dictates specific transcriptional profiles from a limited number of initiating factors. These data were obtained by utilizing a novel technique in FAIRE to assess overall chromatin structure during the process of GR-mediated transcriptional initiation and suggest a preferred transitional chromatin state that allows GR recruitment yet still prevents unregulated transcription.

ACKNOWLEDGMENTS

We offer special thanks to Dan Gilchrist and H. Karimi Kinyamu for critical reading of the manuscript. We express gratitude to Paul Wade for critical analysis of the manuscript and raw T47D input sequence data. We also thank the NIEHS Microarray Facility, NIEHS Next Generation Sequencing Core, and Yuan Gao for their technical support.

This research was supported in part by the Intramural Research Program of the NIH, National Institute of Environmental Health Sciences (Z01 ES071006-11).

REFERENCES

1. **Acevedo ML, Kraus WL.** 2004. Transcriptional activation by nuclear receptors. Essays Biochem. **40**:73–88.
2. **Archer TK, Lefebvre P, Wolford RG, Hager GL.** 1992. Transcription factor loading on the MMTV promoter: a bimodal mechanism for promoter activation. Science **255**:1573–1576.
3. **Archer TK, Zaniewski E, Moyer ML, Nordeen SK.** 1994. The differential capacity of glucocorticoids and progestins to alter chromatin structure and induce gene expression in human breast cancer cells. Mol. Endocrinol. **8**:1154–1162.
4. **Belikov S, Astrand C, Wrange O.** 2009. FoxA1 binding directs chromatin structure and the functional response of a glucocorticoid receptor-regulated promoter. Mol. Cell. Biol. **29**:5413–5425.
5. **Burch JB, Weintraub H.** 1983. Temporal order of chromatin structural changes associated with activation of the major chicken vitellogenin gene. Cell **33**:65–76.
6. **Burd CJ, Kinyamu HK, Miller FW, Archer TK.** 2008. UV radiation regulates Mi-2 through protein translation and stability. J. Biol. Chem. **283**:34976–34982.
7. **Carey MF, Peterson CL, Smale ST.** 2009. Chromatin immunoprecipitation (ChIP). Cold Spring Harb. Protoc. **2009**:pdb.prot5279.
8. **Cirillo LA, et al.** 2002. Opening of compacted chromatin by early developmental transcription factors HNF3 (FoxA) and GATA-4. Mol. Cell **9**:279–289.
9. **Dechassa ML, et al.** 2010. SWI/SNF has intrinsic nucleosome disassembly activity that is dependent on adjacent nucleosomes. Mol. Cell **38**:590–602.
10. **Dilworth FJ, Chambon P.** 2001. Nuclear receptors coordinate the activities of chromatin remodeling complexes and coactivators to facilitate initiation of transcription. Oncogene **20**:3047–3054.
11. **Eeckhoute J, et al.** 2009. Cell-type selective chromatin remodeling defines the active subset of FOXA1-bound enhancers. Genome Res. **19**:372–380.
12. **Evans RM.** 2005. The nuclear receptor superfamily: a Rosetta stone for physiology. Mol. Endocrinol. **19**:1429–1438.
13. **Fryer CJ, Archer TK.** 1998. Chromatin remodelling by the glucocorticoid receptor requires the BRG1 complex. Nature **393**:88–91.
14. **Gevry N, et al.** 2009. Histone H2A. Z is essential for estrogen receptor signaling.Genes Dev. **23**:1522–1533.
15. **Giresi PG, Kim J, McDaniell RM, Iyer VR, Lieb JD.** 2007. FAIRE (Formaldehyde-Assisted Isolation of Regulatory Elements) isolates active regulatory elements from human chromatin. Genome Res. **17**:877–885.
16. **Giresi PG, Lieb JD.** 2009. Isolation of active regulatory elements from eukaryotic chromatin using FAIRE (Formaldehyde Assisted Isolation of Regulatory Elements). Methods **48**:233–239.
17. **Hager GL, et al.** 1993. Influence of chromatin structure on the binding of transcription factors to DNA. Cold Spring Harb Symp. Quant Biol. **58**:63–71.
18. **Hebbar PB, Archer TK.** 2007. Chromatin-dependent cooperativity between site-specific transcription factors in vivo. J. Biol. Chem. **282**:8284–8291.
19. **Heinz S, et al.** 2010. Simple combinations of lineage-determining transcription factors prime cis-regulatory elements required for macrophage and B cell identities. Mol. Cell **38**:576–589.
20. **John S, et al.** 2008. Interaction of the glucocorticoid receptor with the chromatin landscape. Mol. Cell **29**:611–624.
21. **John S, et al.** 2011. Chromatin accessibility pre-determines glucocorticoid receptor binding patterns. Nat. Genet. **43**:264–268.
22. **Kininis M, Kraus WL.** 2008. A global view of transcriptional regulation by nuclear receptors: gene expression, factor localization, and DNA sequence analysis. Nucl. Recept. Signal. **6**:e005.
23. **Lander ES, et al.** 2001. Initial sequencing and analysis of the human genome. Nature **409**:860–921.
24. **Langmead B, Trapnell C, Pop M, Salzberg SL.** 2009. Ultrafast and memory-efficient alignment of short DNA sequences to the human genome. Genome Biol. **10**:R25.
25. **Lee HL, Archer TK.** 1994. Nucleosome-mediated disruption of transcription factor-chromatin initiation complexes at the mouse mammary tumor virus long terminal repeat in vivo. Mol. Cell. Biol. **14**:32–41.
26. **Lee KC, Lee Kraus W.** 2001. Nuclear receptors, coactivators and chromatin: new approaches, new insights. Trends Endocrinol. Metab. **12**:191–197.
27. **McDonnell DP, Wardell SE.** 2010. The molecular mechanisms underlying the pharmacological actions of ER modulators: implications for new drug discovery in breast cancer. Curr. Opin. Pharmacol. **10**:620–628.
28. **Muchardt C, Yaniv M.** 1993. A human homologue of Saccharomyces cerevisiae SNF2/SWI2 and Drosophila brm genes potentiates transcriptional activation by the glucocorticoid receptor. EMBO J. **12**:4279–4290.
29. **Owen-Hughes T, Utley RT, Cote J, Peterson CL, Workman JL.** 1996. Persistent site-specific remodeling of a nucleosome array by transient action of the SWI/SNF complex. Science **273**:513–516.
30. **Peterson CL, Tamkun JW.** 1995. The SWI-SNF complex: a chromatin remodeling machine? Trends Biochem. Sci. **20**:143–146.
31. **R Development Core Team.** 2011. R: a language and environment for statistical computing. R Foundation for Statistical Computing, Vienna, Austria.
32. **Reddy TE, et al.** 2009. Genomic determination of the glucocorticoid response reveals unexpected mechanisms of gene regulation. Genome Res. **19**:2163–2171.
33. **Reik A, Schutz G, Stewart AF.** 1991. Glucocorticoids are required for establishment and maintenance of an alteration in chromatin structure: induction leads to a reversible disruption of nucleosomes over an enhancer. EMBO J. **10**:2569–2576.
34. **Sharp ZD, et al.** 2006. Estrogen-receptor-alpha exchange and chromatin dynamics are ligand- and domain-dependent. J. Cell Sci. **119**:4101–4116.
35. **Stafford JM, Wilkinson JC, Beechem JM, Granner DK.** 2001. Accessory factors facilitate the binding of glucocorticoid receptor to the phosphoenolpyruvate carboxykinase gene promoter. J. Biol. Chem. **276**:39885–39891.
36. **Trotter KW, Archer TK.** 2008. The BRG1 transcriptional coregulator. Nucl. Recept Signal. **6**:e004.
37. **Trotter KW, Archer TK.** 2004. Reconstitution of glucocorticoid receptor-dependent transcription in vivo. Mol. Cell. Biol. **24**:3347–3358.
38. **Trotter KW, Fan HY, Ivey ML, Kingston RE, Archer TK.** 2008. The HSA domain of BRG1 mediates critical interactions required for glucocorticoid receptor-dependent transcriptional activation in vivo. Mol. Cell. Biol. **28**:1413–1426.
39. **Truss M, Bartsch J, Mows C, Chavez S, Beato M.** 1996. Chromatin structure of the MMTV promoter and its changes during hormonal induction. Cell. Mol. Neurobiol. **16**:85–101.
40. **Tsai CC, Fondell JD.** 2004. Nuclear receptor recruitment of histone-modifying enzymes to target gene promoters. Vitam. Horm. **68**:93–122.
41. **Voss TC, et al.** 2011. Dynamic exchange at regulatory elements during chromatin remodeling underlies assisted loading mechanism. Cell **146**:544–554.
42. **Wolf IM, Heitzer MD, Grubisha M, DeFranco DB.** 2008. Coactivators and nuclear receptor transactivation. J. Cell Biochem. **104**:1580–1586.

43. **Xi H, et al.** 2007. Identification and characterization of cell type-specific and ubiquitous chromatin regulatory structures in the human genome. PLoS Genet. **3**:e136.
44. **Yoshinaga SK, Peterson CL, Herskowitz I, Yamamoto KR.** 1992. Roles of SWI1, SWI2, and SWI3 proteins for transcriptional enhancement by steroid receptors. Science **258**:1598–1604.
45. **Zaret KS, Yamamoto KR.** 1984. Reversible and persistent changes in chromatin structure accompany activation of a glucocorticoid-dependent enhancer element. Cell **38**:29–38.
46. **Zhou VW, Goren A, Bernstein BE.** 2011. Charting histone modifications and the functional organization of mammalian genomes. Nat. Rev. Genet. **12**:7–18.